Relating High-Energy Lepton-Hadron, Proton-Nucleus, and Nucleus-Nucleus Collisions through Geometric Scaling

Néstor Armesto, Carlos A. Salgado, and Urs Achim Wiedemann
Department of Physics, CERN, Theory Division, CH-1211 Genève 23, Switzerland
(Received 14 July 2004; published 20 January 2005)

A characteristic feature of small-x lepton-proton data from HERA is geometric scaling: the fact that in the region of small Bjorken variable x, $x \lesssim 0.01$, all data can be described by a single variable $Q^2/Q^2_{s,p}(x)$, with all x dependence encoded in the so-called saturation momentum $Q_{s,p}(x)$. Here, we observe that the same scaling ansatz accounts for nuclear photoabsorption cross sections and favors the nuclear dependence $Q^2_{s,A} \propto A^\alpha Q^2_{s,p}$, $\alpha \simeq 4/9$. We then make the empirical finding that the same A dependence accounts for the centrality evolution of the multiplicities measured in Au + Au collisions at RHIC. It also allows one to parametrize the high-p_t particle suppression in d + Au collisions at forward rapidities. If these geometric scaling properties have a common dynamical origin, then this A dependence of $Q^2_{s,A}$ should emerge as a consequence of the underlying dynamical model.

DOI: 10.1103/PhysRevLett.94.022002 PACS numbers: 13.60.Hb, 12.38.Cy

All data for the photoabsorption cross section $\sigma^{\gamma^* p}(x, Q^2)$ in lepton-proton scattering with $x \leq 0.01$ have been found [1] to lie on a single curve when plotted against the variable $Q^2/Q^2_{s,p}$, with $Q^2_{s,p} \sim x^{-\lambda}$ and $\lambda \simeq 0.3$. To further explore this empirical property of *geometric scaling*, we study here how experimental data on lepton-nucleus collisions constrain the geometric information entering the saturation scale. We also ask to what extent the geometric scaling ansatz can account for characteristic features of particle production in other nuclear collision systems.

Geometric scaling is usually motivated in the QCD dipole model [2] where the total $\gamma^* h$ cross section reads

$$\sigma^{\gamma^* h}_{T,L}(x, Q^2) = \int d\mathbf{r} \int_0^1 dz |\Psi^{\gamma^*}_{T,L}(Q^2, \mathbf{r}, z)|^2 \sigma^h_{\rm dip}(\mathbf{r}, x). \quad (1)$$

Here $\Psi_{T,L}$ are the perturbatively computed transverse and longitudinal wave functions for the splitting of γ^* into a $q\bar{q}$ dipole of transverse size $\mathbf{r}$ with light-cone fractions z and $(1-z)$ carried by the quark and the antiquark, respectively. Both for a proton ($h = p$) and for a nucleus ($h = A$), $\sigma^h_{\rm dip}(\mathbf{r}, x)$ can be written as an integral of the dipole scattering amplitude N_h over the impact parameter $\mathbf{b}$,

$$\sigma^h_{\rm dip}(\mathbf{r}, x) = 2 \int d\mathbf{b} N_h(\mathbf{r}, x; \mathbf{b}). \quad (2)$$

In this setting, geometric scaling corresponds to the condition $N_h(\mathbf{r}, x; \mathbf{b}) \equiv N_h(r Q_{s,h}(x, \mathbf{b}))$. This can be seen by rescaling the impact parameter in (2) in terms of the radius R_h of the hadronic target, $\bar{\mathbf{b}} = \mathbf{b}/\sqrt{\pi R_h^2}$,

$$\sigma^{\gamma^* h}_{T,L}(x, Q^2) = \pi R_h^2 \int d\mathbf{r} \int_0^1 dz |\Psi^{\gamma^*}_{T,L}(Q^2, \mathbf{r}, z)|^2 \times 2 \int d\bar{\mathbf{b}} N_h(r Q_{s,h}(x, \bar{\mathbf{b}})). \quad (3)$$

For a trivial impact-parameter dependence of the saturation scale, $Q_{s,h}(x, \mathbf{b}) = Q_{s,h}(x)\Theta(R_h - b)$, and since $|\Psi^{\gamma^*}_{T,L}(Q^2, \mathbf{r}, z)|^2$ is proportional to Q^2 times a function of $\mathbf{r}^2 Q^2$, Eq. (3) depends solely on $\tau_h = Q^2/Q^2_{s,h}(x)$. For realistic functional shapes of the form $Q_{s,h}(x, \mathbf{b}) \propto f(b/R_h)$, the same τ dependence results if $Q^2_{s,h}(x)$ is defined as an appropriate $\mathbf{b}$ average of $Q^2_{s,h}(x, \mathbf{b})$. In the case of $\gamma^* A$ interactions, geometric scaling is the property that the A dependence of the ratio $\sigma^{\gamma^* A}_{T,L}/\pi R_A^2$ can be absorbed in the A dependence of this impact-parameter independent saturation scale $Q_{s,A}(x)$,

$$\frac{\sigma^{\gamma^* A}(\tau_A)}{\pi R_A^2} = \frac{\sigma^{\gamma^* p}(\tau_A)}{\pi R_p^2}. \quad (4)$$

For this A dependence, we make the ansatz that the saturation scale in the nucleus grows with the quotient of the transverse parton densities to the power $1/\delta$,

$$Q^2_{s,A} = Q^2_{s,p}\left(\frac{A \pi R_p^2}{\pi R_A^2}\right)^{1/\delta} \Rightarrow \tau_A = \tau_p\left(\frac{\pi R_A^2}{A \pi R_p^2}\right)^{1/\delta}, \quad (5)$$

where the nuclear radius is given by the usual parametrization $R_A = (1.12 A^{1/3} - 0.86 A^{-1/3})$ fm. We treat δ and πR_p^2 as free parameters to be fixed by data.

In Fig. 1 we plot the experimental $\gamma^* p$ data [3] with $x \leq 0.01$ as a function of $\tau_p = Q^2/Q^2_{s,p}$. For $Q^2_{s,p}$, we use in this plot the Golec-Biernat and Wüsthoff (GBW) parametrization [4] with $Q^2_{s,p} = (\bar{x}/x_0)^{-\lambda}$ in GeV^2, $x_0 = 3.04 \times 10^{-4}$, and $\lambda = 0.288$. To extend to low virtuality, the x dependence of the GBW parametrization is modified by a mass term $\bar{x} = x[(Q^2 + 4m_f^2)/Q^2]$, with $m_f = 0.14$ GeV. The data [3] are seen to be parametrized well by the scaling curve

$$\sigma^{\gamma^* p}(x, Q^2) \equiv \Phi(\tau_p) = \bar{\sigma}_0[\gamma_E + \Gamma(0, \xi) + \ln\xi], \quad (6)$$

where γ_E is the Euler constant, $\Gamma(0, \xi)$ is the incomplete Γ function, and $\xi = a/\tau_p^b$, with $a = 1.868$ and $b = 0.746$. The normalization is fixed by $\bar{\sigma}_0 = 40.56$ mb. Assuming in the GBW model that the b dependence of $Q^2_{s,h}$ is a

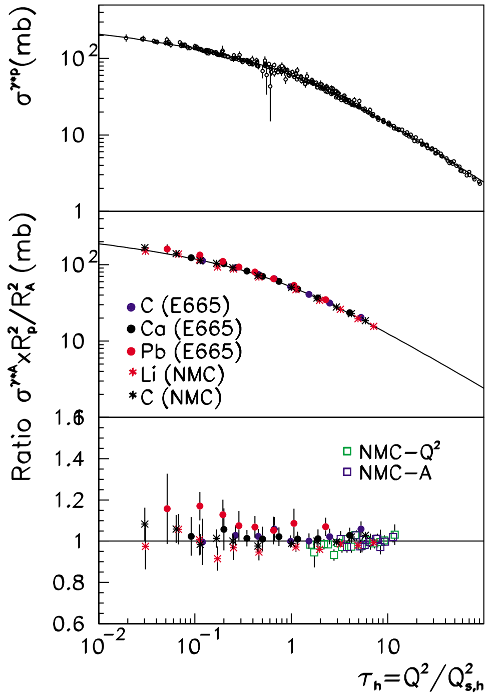

FIG. 1 (color online). Geometric scaling for $\gamma^* p$ (upper panel, data from [3]), $\gamma^* A$ (middle panel, data from [5,6]), and the ratio of data for $\gamma^* A$ over the prediction from (6) (lower panel). As an additional check, the lower plot also shows data for $\gamma^* A$ normalized with respect to $\gamma^* C$ [7] and divided by the corresponding prediction from Eq. (6).

Gaussian, and approximating $|\Psi^{\gamma^*}|^2 \propto \delta^{(2)}(\mathbf{r}^2 - 4/Q^2)$, one obtains the functional shape (6) from (3). For our purpose, however, Eq. (6) is just a convenient ansatz for the scaling function $\Phi(\tau_h)$.

To determine $Q^2_{s,A}$, we compare the functional shape of (6) to the available experimental data for $\gamma^* A$ collisions with $x \le 0.0175$ [5–7], using $\xi = a/\tau_A^b$. The parameters δ and πR_p^2 in (4)–(6) are fitted by χ^2 minimization adding the statistical and systematic errors in quadrature. The data sets [5–7] have additional normalization errors of 0.4%, 0.2%, and 0.15%; the quality of the fit improves by multiplying the data by the factors 1.004, 1.002, and 0.9985, respectively. We obtain $\delta = 0.79 \pm 0.02$ and $\pi R_p^2 = 1.55 \pm 0.02$ fm^2 for a χ^2/d.o.f. $= 0.95$; see Fig. 1 for comparison. If the normalizations are all set to 1, we obtain an almost identical fit with $\delta = 0.80 \pm 0.02$ and $\pi R_p^2 = 1.57 \pm 0.02$ fm^2 for a χ^2/d.o.f. $= 1.02$. If we impose $\delta = 1$ in the fit, which corresponds to $Q^2_{s,A} \propto A^{1/3}$ for large nuclei, a much worse value of χ^2/d.o.f. $= 2.35$ is obtained. We conclude that the small-x experimental data on $\gamma^* A$ collisions favor an increase of $Q^2_{s,A}$ faster than $A^{1/3}$. The numerical coincidence $b \simeq \delta$ is consistent with the absence of shadowing in nuclear parton distributions at $Q^2 \gg Q^2_{s,A}$.

Can geometric scaling and, in particular, the A dependence and energy dependence of $Q_{s,A}(x)$ account for the p_t-integrated multiplicity in symmetric nucleus-nucleus collisions at midrapidity? To address this question, we turn now to the heuristic ansatz

$$\frac{dN^{AA}}{dy}\bigg|_{y\sim 0} \propto Q^2_{s,A}\pi R_A^2, \tag{7}$$

which arises in several models of hadroproduction [8–11]. These models relate the parton distribution measured in $\sigma^{\gamma^* A}$ to the hadroproduction measured in nucleus-nucleus collisions. For example, the factorized formula [8] calculates gluon production by convoluting A-dependent gluon distribution functions:

$$\frac{dN_g^{AB}}{dyd\mathbf{p}_t d\mathbf{b}} \propto \frac{\alpha_S}{\mathbf{p}_t^2}\int d\mathbf{k}\,\phi_A(y, \mathbf{k}^2, \mathbf{b})\phi_B(y, (\mathbf{k}-\mathbf{p}_t)^2, \mathbf{b}), \tag{8}$$

where $\phi_h(y, \mathbf{k}, \mathbf{b}) = \int d\mathbf{r}\exp\{i\mathbf{r}\cdot\mathbf{k}\}N_h(\mathbf{r}, x; \mathbf{b})/(2\pi r^2)$ [9], and $y = \ln 1/x$. For geometric scaling, $\phi_A(y, \mathbf{k}^2, \mathbf{b}) \equiv \phi(\mathbf{k}^2/Q^2_{s,A}(y, \mathbf{b}))$, we find the dependence of Eq. (7),

$$\frac{dN_g^{AA}}{dy}\bigg|_{y\sim 0} \propto \int \frac{d\mathbf{p}_t}{\mathbf{p}_t^2} d\mathbf{k}\, d\mathbf{b}\,\phi\Big(\frac{\mathbf{k}^2}{Q^2_{s,A}}\Big)\phi\Big(\frac{(\mathbf{k}-\mathbf{p}_t)^2}{Q^2_{s,A}}\Big)$$
$$= Q^2_{s,A}\pi R_A^2 \int \frac{d\mathbf{s}}{\mathbf{s}^2} d\tau\, d\bar{\mathbf{b}}\,\phi(\tau^2)\phi((\tau-\mathbf{s})^2). \tag{9}$$

Also without invoking factorization in (8), any integrand with $(k/Q_{s,A})$ scaling leads to Eq. (7); see [10,11]. In all these models, the hadron yield is assumed to be proportional to the yield of produced partons.

The energy dependence of (7) is given by the GBW parameter $\lambda = 0.288$. For the centrality dependence of (7), we use the known proportionality in symmetric $A + A$ collisions between the number $N_{\rm part}$ of participant nucleons and the nuclear size A. With $Q^2_{s,A} \propto A^{1/3\delta}$, and $\delta = 0.79 \pm 0.02$, we thus obtain

$$\frac{1}{N_{\rm part}}\frac{dN^{AA}}{d\eta}\bigg|_{\eta\sim 0} = N_0\sqrt{s}^\lambda N_{\rm part}^{(1-\delta)/3\delta}. \tag{10}$$

As seen in Fig. 2, this ansatz accounts for experimental data from the PHOBOS Collaboration [12] on charged multiplicities in Au + Au collisions at $\sqrt{s} = 19.6$, 130, and 200 GeV/A. Even the $\bar{p} + p$ data ([13], as quoted in [12]) at $\sqrt{s} = 19.6$ and 200 GeV are accounted for by Eq. (10). Since all data are at midrapidity, the Jacobian between rapidity y and pseudorapidity η is approximately constant. It has been absorbed in the overall normalization $N_0 = 0.47$ which is independent of the energy and the centrality of the collision. Figure 2 also shows the result of (10) for intermediate Relativistic Heavy-Ion Collider (RHIC) energy ($\sqrt{s} = 62.5$ GeV/A), for Large Hadron Collider (LHC) energy ($\sqrt{s} = 5500$ GeV/A) and for smaller colliding nuclei. Equation (10) implies that the energy and the centrality dependence of the multiplicity factorize, in agreement with the results by PHOBOS [12].

In the current debate of RHIC data on the suppressed high-p_t hadroproduction in nuclear collisions, the rele-

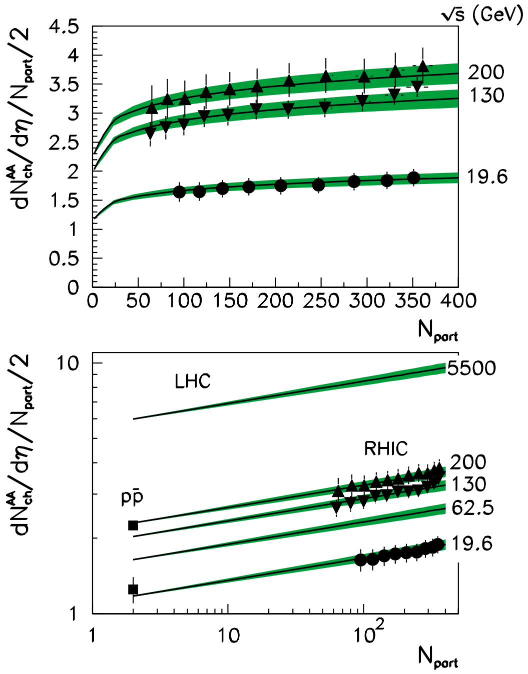

FIG. 2 (color online). Energy and centrality dependence of the multiplicity of charged particles in Au + Au collisions (10) compared to PHOBOS data [12]. Also shown in the lower panel are the $\bar{p}+p$ data [13] and results for $\sqrt{s}=62.5$ and 5500 GeV/A.

vance of nuclear shadowing has been discussed repeatedly [14,15]. It is clear by now [16] that the A dependence of p_t-differential hadroproduction in nucleus-nucleus collisions and in deuteron-nucleus collisions at midrapidity both involve additional nuclear effects which are at least as significant as nuclear shadowing. On the other hand, arguments have been put forward [14,15] that in d + Au collisions at forward rapidity nuclear shadowing may be the dominant effect. Motivated by the phenomenological success of the scaling ansatz (10), we now test to what extent the centrality dependence of p_t-differential hadron spectra in d + Au emerges naturally from the geometric scaling found in $\gamma^* A$. We use Eq. (8) with the ansatz $\phi_A(k=Q/2) \simeq \Phi(\tau_A)$ such that $\tau_A = k^2/4\bar{Q}^2_{s,A}$, where now the gluon saturation scale $\bar{Q}^2_{s,A} = N_c Q^2_{s,A}/C_F$ is employed. The approximation $\phi(k=Q/2) \simeq \Phi(\tau_A)$ has been checked numerically. The parton distribution in the deuteron is taken to fall off sufficiently quickly, $\phi_d \sim 1/k_t^n$, $n \gg 1$, so that we can write for the centrality classes c_1, c_2,

$$\frac{dN^{d\mathrm{Au}}_{c_1}}{N_{\mathrm{coll}_1} d\eta d^2 p_t} \Big/ \frac{dN^{d\mathrm{Au}}_{c_2}}{N_{\mathrm{coll}_2} d\eta d^2 p_t} \approx \frac{N_{\mathrm{coll}_2} \phi_A(p_t/Q_{s,c_1})}{N_{\mathrm{coll}_1} \phi_A(p_t/Q_{s,c_2})} \approx \frac{N_{\mathrm{coll}_2} \Phi(\tau_{c_1})}{N_{\mathrm{coll}_1} \Phi(\tau_{c_2})}. \tag{11}$$

We see the use of this pocket formula mainly in emphasizing the plausible claim that the suppression of d + Au at forward rapidity traces directly the suppression of nuclear parton distributions at small x. For the comparison in Fig. 3 to data [17] on the normalized yields of central and semicentral over peripheral d + Au collisions, we use the number of nucleon-nucleon collisions N_{coll} in different centrality bins [17] with $N_{\mathrm{coll}_1} = 13.6 \pm 0.3$, 7.9 ± 0.4 and $N_{\mathrm{coll}_2} = 3.3 \pm 0.4$. Only the two most forward rapidities $\eta = 2.2$ and 3.2 are compared. We find that Eq. (11) captures the main features of the recent data by BRAHMS [17], but it shows a weaker rapidity dependence. A more quantitative discussion is certainly beyond the accuracy of (11). The only conclusion from this exercise is that the more differential analysis of (8) is not inconsistent with data in d + Au.

We now comment on the differences with other approaches. The geometric scaling in $\gamma^* A$ data has been studied in [18], where a growth of $Q^2_{s,A} \propto A^\alpha$, $\alpha \leq 1/3$, has been found. This disagreement with our finding could have several origins. First, $0.01 < x < 0.1$ was allowed in [18]; however, in this antishadowing region, we find no scaling in the data, as expected. Moreover, [18] does not modify the variable $\bar{x}$ for small Q^2 as done in this work and in the GBW model. Second, [18] uses $R_A \propto A^{1/3}$, which leads to differences, in particular, for small A; we find a much worse fit in terms of χ^2 for such an ansatz. In [18] this disagreement is improved by introducing a free parameter γ in the A-dependent normalization of the nuclear F_2^A data, $A^{-\gamma-1}$. In our case, however, this normalization is fixed by a dimensional quantity given by the scaling condition (4).

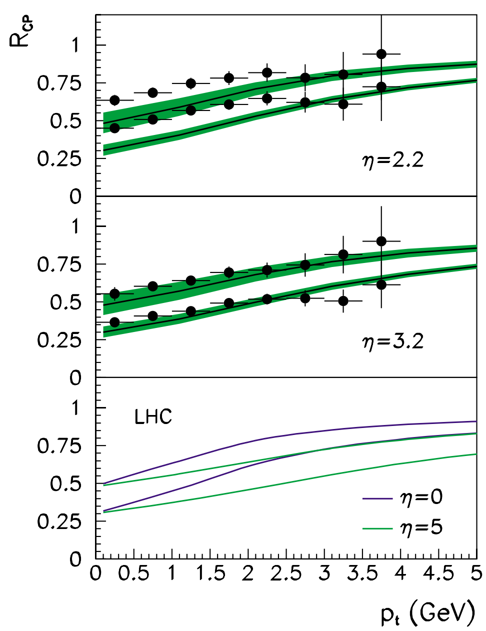

FIG. 3 (color online). Normalized ratios of central and semicentral to peripheral d + Au collisions measured by BRAHMS [17] compared to results from Eq. (11). The bands represent the uncertainty in the determination of N_{coll} [17]. Results for the same centrality classes at the LHC are given in the lower panel.

The multiplicities in Au + Au collisions at RHIC have been studied [19] on the basis of Eq. (8) assuming $Q_{s,A}^2 \propto A^{1/3}$. These authors are led to an expression which is Eq. (10) with $\delta = 1$ times an additional factor $\ln(\sqrt{s}^{\lambda} N_{\rm part}^{1/3})$ argued to come from scaling violations. We note that, for the accessible range of A, $A^{4/9} \sim A^{1/3}\ln(A^{1/3})$; this is the reason why both approaches provide a fair description of the data at RHIC. However, the energy dependence in the logarithmic prefactor introduced in [19] implies a flatter centrality dependence with increasing energy.

Finally, the connection between the small x and the A dependence of parton distribution functions, and the suppression of normalized yields in d + Au collisions [17] at forward rapidity, has been discussed in several recent works [14,15]. Equation (11) contributes to this discussion by illustrating to what extent the suppression of high-p_t particles in d + Au at RHIC can be accounted for by the shadowing in $\gamma^* A$ collisions; see Eq. (6).

Here we have discussed to what extent data for different collision systems in $\gamma^* A$, d + Au, and $A + A$ can be related through geometric scaling. Our study does not exclude the possibility that geometric scaling in $\gamma^* p$ and $\gamma^* A$ is a numerical coincidence without any dynamical origin. However, nonlinear small-x QCD evolution equations [20,21] allow one to absorb the entire dependence of small-x parton distributions on energy and geometry into a single quantity, $Q_{s,h}$. The data discussed here are currently regarded [16] as the main support for such nonlinear saturation effects. In fact, the scaling function Φ in (6) resembles the asymptotic solution of the Balitsky-Kovchegov (BK) equation: it behaves as $\ln(k/Q_{s,p})$ $[(Q_{s,p}^2/k^2)^b]$ for small [large] k [14,22]. Given that these nonlinear evolution equations hold in a novel high-density regime of QCD which may become experimentally accessible, it is of obvious interest to ask whether the connection between geometric scaling in the theory and in the data can be made more quantitative. On the theoretical side, this requires at least the study of the impact-parameter dependence [23] of small-x evolution and the control of higher order effects. In particular, running coupling effects are known qualitatively to decrease the energy dependence [24] and the A dependence [25] of the saturation scale in comparison to the BK equation at fixed coupling. While an A dependence of $Q_{s,A}^2 \propto A^{1/3}$ is often assumed [26], much stronger ones (such as $\alpha \simeq 2/3$ [27]) have also been proposed. The present work has analyzed to what extent data constrain these energy and A dependences. These constraints have to be met by nonlinear small-x evolution or by any other model which aims at providing the common dynamical origin for geometric scaling in different nuclear collisions.

We thank R. Baier, M. Braun, A. Capella, D. Kharzeev, A. Kovner, L. McLerran, G. Roland, K. Rummukainen, and H. Weigert for discussions.

[1] A. M. Stasto, K. Golec-Biernat, and J. Kwiecinski, Phys. Rev. Lett. **86**, 596 (2001).

[2] N. N. Nikolaev and B. G. Zakharov, Z. Phys. C **49**, 607 (1991); A. H. Mueller, Nucl. Phys. **B415**, 373 (1994).

[3] J. Breitweg *et al.*, Phys. Lett. B **487**, 53 (2000); C. Adloff *et al.*, Eur. Phys. J. C **21**, 33 (2001); C. Adloff *et al.*, Nucl. Phys. **B497**, 3 (1997); M. R. Adams *et al.*, Phys. Rev. D **54**, 3006 (1996).

[4] K. Golec-Biernat and M. Wüsthoff, Phys. Rev. D **59**, 014017 (1999).

[5] M. R. Adams *et al.*, Z. Phys. C **67**, 403 (1995).

[6] M. Arneodo *et al.*, Nucl. Phys. **B441**, 12 (1995).

[7] M. Arneodo *et al.*, Nucl. Phys. **B481**, 3 (1996); **B481**, 23 (1996).

[8] L. V. Gribov, E. M. Levin, and M. G. Ryskin, Phys. Rep. **100**, 1 (1983).

[9] M. A. Braun, Phys. Lett. B **483**, 105 (2000); Y. V. Kovchegov and K. Tuchin, Phys. Rev. D **65**, 074026 (2002); R. Baier, A. H. Mueller, and D. Schiff, Nucl. Phys. **A741**, 358 (2004).

[10] Y. V. Kovchegov, Nucl. Phys. **A692**, 557 (2001).

[11] K. J. Eskola, K. Kajantie, P. V. Ruuskanen, and K. Tuominen, Nucl. Phys. **B570**, 379 (2000).

[12] PHOBOS Collaboration, B. B. Back *et al.*, Phys. Rev. C **65**, 061901 (2002); **70**, 021902 (2004).

[13] W. Thome *et al.*, Nucl. Phys. **B129**, 365 (1977); G. J. Alner *et al.*, Z. Phys. C **33**, 1 (1986).

[14] J. L. Albacete *et al.*, Phys. Rev. Lett. **92**, 082001 (2004).

[15] D. Kharzeev, E. Levin, and L. McLerran, Phys. Lett. B **561**, 93 (2003); R. Baier, A. Kovner, and U. A. Wiedemann, Phys. Rev. D **68**, 054009 (2003); D. Kharzeev, Y. V. Kovchegov, and K. Tuchin, Phys. Rev. D **68**, 094013 (2003); hep-ph/0405045.

[16] M. Gyulassy and L. McLerran, nucl-th/0405013.

[17] BRAHMS Collaboration, I. Arsene *et al.*, Phys. Rev. Lett. **93**, 242303 (2004).

[18] A. Freund, K. Rummukainen, H. Weigert, and A. Schafer, Phys. Rev. Lett. **90**, 222002 (2003).

[19] D. Kharzeev and M. Nardi, Phys. Lett. B **507**, 121 (2001); D. Kharzeev and E. Levin, Phys. Lett. B **523**, 79 (2001).

[20] I. Balitsky, Nucl. Phys. **B463**, 99 (1996); Y. V. Kovchegov, Phys. Rev. D **60**, 034008 (1999).

[21] N. Armesto and M. A. Braun, Eur. Phys. J. C **20**, 517 (2001); M. Lublinsky, Eur. Phys. J. C **21**, 513 (2001); S. Munier and R. Peschanski, Phys. Rev. Lett. **91**, 232001 (2003); Phys. Rev. D **70**, 077503 (2004).

[22] E. Iancu, K. Itakura, and L. McLerran, Nucl. Phys. **A708**, 327 (2002); A. H. Mueller and D. N. Triantafyllopoulos, Nucl. Phys. **B640**, 331 (2002).

[23] K. Golec-Biernat and A. M. Stasto, Nucl. Phys. **B668**, 345 (2003); E. Gotsman *et al.*, Nucl. Phys. **A742**, 55 (2004).

[24] D. N. Triantafyllopoulos, Nucl. Phys. **B648**, 293 (2003); M. A. Braun, Phys. Lett. B **576**, 115 (2003).

[25] A. H. Mueller, Nucl. Phys. **A724**, 223 (2003); K. Rummukainen and H. Weigert, Nucl. Phys. **A739**, 183 (2004).

[26] L. D. McLerran and R. Venugopalan, Phys. Rev. D **49**, 2233 (1994); **49**, 3352 (1994).

[27] Y. V. Kovchegov, Phys. Rev. D **61**, 074018 (2000); E. Levin and K. Tuchin, Nucl. Phys. **B573**, 833 (2000).